Title

Targeted Quantitative Kinome Analysis Identifies PRPS2 as a Promoter for Colorectal Cancer Metastasis.

Journal

Journal of Proteome Research, 18(5)

Authors

Wang, Yinsheng
Miao, Weili

Publication Date

2019-05-03

DOI

10.1021/acs.jproteome.9b00119

Peer reviewed

HHS Public Access
Author manuscript
J Proteome Res. Author manuscript; available in PMC 2020 May 03.

Published in final edited form as:
J Proteome Res. 2019 May 03; 18(5): 2279–2286. doi:10.1021/acs.jproteome.9b00119.

Targeted Quantitative Kinome Analysis Identifies PRPS2 as a Promoter for Colorectal Cancer Metastasis

Weili Miao and **Yinsheng Wang***
Department of Chemistry, University of California, Riverside, California 92521-0403, United States

Abstract

Kinases are among the most important families of enzymes involved in cell signaling. In this study, we employed a recently developed parallel-reaction monitoring (PRM)-based targeted proteomic method to examine the reprogramming of the human kinome during colorectal cancer (CRC) metastasis. We were able to quantify the relative expression of 299 kinase proteins in a pair of matched primary/metastatic CRC cell lines. We also found that, among the differentially expressed kinases, phosphoribosyl pyrophosphate synthetase 2 (PRPS2) promotes the migration and invasion of cultured CRC cells through regulating the activity of matrix metalloproteinase 9 (MMP-9) and the expression of E-cadherin. Moreover, we found that the up-regulation of PRPS2 in metastatic CRC cells could be induced by the *MYC* proto-oncogene. Together, our unbiased kinome profiling approach led to the identification, for the first time, of PRPS2 as a promoter for CRC metastasis.

Graphical Abstract

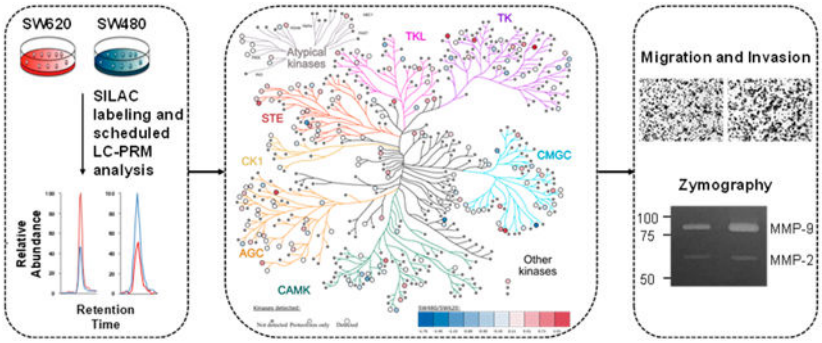

***Corresponding Author** yinsheng.wang@ucr.edu. Phone: (951)827-2700.

Supporting Information
The Supporting Information is available free of charge on the ACS Publications website at DOI: 10.1021/acs.jproteo-me.9b00119.
Relative expression levels of kinases; sequences for RT-qPCR primers; extracted-ion chromatograms; pathway analysis; Western blot image and quantificaiton results; real-time PCR results; Myc drives expression of PRPS2 in CRC cells and patients; schematic diagram showing Myc-mediated expression of PRPS2 in CRC metastasis (PDF)
Supporting peptide data (XLSX)

The authors declare no competing financial interest.
All the raw files for LC-PRM analyses of kinases for the paired colon cancer cells were deposited into PeptideAtlas with the identifier number of PASS01256 (http://www.peptideatlas.org/PASS/PASS01256).

Keywords

quantitative proteomics; parallel-reaction monitoring; SILAC; kinase; kinome; colorectal cancer; metastasis; PRPS2; Myc; matrix metalloproteinase

INTRODUCTION

Colorectal cancer (CRC) is a major cause of morbidity and mortality throughout the world. It accounts for over 9% of all cancer incidences, ranks as the third most frequently diagnosed cancer worldwide, and ranks fourth among the cancer-related deaths.[1] Metastases are the main cause of cancer-related mortality in CRC patients,[2] where approximately half of CRC patients develop metastatic disease[3] and the 5-year survival rate for metastatic CRC (stage IV) is less than 10%.[4]

Aberrant kinase expression is known to be associated with CRC metastasis. For example, CRC patients with elevated EGFR expression exhibit poor prognosis,[5] and overexpression of AXL promotes the migration and invasion in CRC.[6] Thus, a comprehensive analysis of kinase protein expression during CRC metastasis may allow for a systematic understanding about the implications of kinases in modulating the metastatic transformation of CRC.

Several quantitative proteomic methods were recently reported for the interrogation of the whole human kinome. For instance, ATP-acyl nucleotide affinity probes could be employed for the enrichment and quantification of kinases by liquid chromatography-multiple-reaction monitoring (LC-MRM) analysis.[7–9] In this approach, the labeling of a kinase by the ATP affinity probe can be modulated by both the protein expression level and the ATP-binding affinity of the kinase.[14] Likewise, enrichment of kinases relying on the use of affinity resin immobilized with multiple kinase inhibitors may also be affected by changes in kinase activity.[10–13]

We recently developed a parallel-reaction monitoring (PRM)-based targeted proteomic method to analyze the kinase protein expression at the entire proteome scale, and we also applied successfully the method for assessing the reprogramming of the human kinome upon treatment with a kinase inhibitor.[14] In this respect, we established a Skyline kinome library for LC-PRM analysis based on shotgun proteomic data acquired from indepth LC–MS/MS analyses of tryptic digestion mixtures of protein lysates from multiple human cell lines.[14] The library encompassed 1050 tryptic peptides representing 478 kinase proteins, among which 395 are protein kinases.[14]

In this study, we employed the LC-PRM method to profile the differential protein expression of kinases in a pair of primary/metastatic CRC cells initiated from the same patient. We were able to quantify the expression of 299 unique kinases and identify PRPS2 as a driver for CRC metastasis.

EXPERIMENTAL SECTION

Cell Culture

SW480 (primary) and SW620 (metastatic) (ATCC) cells were cultured in Dulbecco's modified Eagle medium (DMEM). Culture media were supplemented with 10% fetal bovine serum (Invitrogen, Carlsbad, CA) and penicillin (100 IU/mL). The cells were maintained at 37 °C in a humidified atmosphere containing 5% CO_2. Approximately 2×10^7 cells were harvested, washed with cold PBS for three times, and lysed by incubating on ice for 30 min with CelLytic M cell lysis reagent (Sigma) containing 1% protease inhibitor cocktail. The cell lysates were centrifuged at 9000g at 4 °C for 30 min and the resulting supernatants collected. For SILAC labeling experiments, the cells were cultured in SILAC medium containing unlabeled lysine and arginine or [$^{13}C_6$, $^{15}N_2$]-lysine and [$^{13}C_6$]-arginine for at least five cell doublings.

Plasmids and shRNAs

The cDNA sequence of *PRPS2* gene was PCR-amplified from a cDNA library prepared from mRNA isolated from SW620 cells, and the primers were 5′-ATGCCCAACATCGTGCTGTT-3′ and 5′-TAGCGGGACATGGCTGAACA-3′. The cDNA was subcloned into *Bam*HI- and XbaI-linearized pRK7 vector. pRK7-PRPS2 and empty pRK7 vectors were transfected into SW480 cells by using Transit-2020 (Mirus). All shRNA targeting sequences, which were designed according to Sigma (https://www.sigmaaldrich.com/life-science/functional-genomics-and-rnai/shrna/individual-genes.html), were cloned into pLKO.1-Puro (Addgene). The sequences for shPRPS2 were 5′-CCATACGCCCGACAAGATAAA-3′ (shPRPS2–1) and 5′-GTCACAAACACAATTCCGCAA-3′ (shPRPS2–2); and scrambled control sequence: 5′-TCCTAAGGTTAAGTCGCCCTCG-3′.

Lentiviral particles were packaged using HEK293T cells. Virus-containing supernatants were collected at 48 h following transfection and filtered to eliminate cells. SW620 cells were infected with the lentivirus for 48 h prior to puromycin (1.0 μg/mL) selection.

Tryptic Digestion of Whole-Cell Protein Lysates

The protein lysates prepared from SW480 and SW620 cells were quantified using Bradford assay (Bio-Rad) and combined at 1:1 ratio (by mass), washed with 8 M urea for protein denaturation, and then treated with dithiothreitol and iodoacetamide for cysteine reduction and alkylation, respectively. The proteins were subsequently digested with modified MS-grade trypsin (Pierce) at an enzyme/substrate ratio of 1:100 in 50 mM NH_4HCO_3 (pH 8.5) at 37 °C overnight. The peptide mixture was subsequently dried in a Speed-vac, desalted with OMIX C18 pipet tips (Agilent Technologies), and subjected to LC–MS/MS analysis in the PRM mode.

LC-PRM Analysis

All scheduled LC-PRM experiments were carried out on a Q Exactive Plus quadrupole-Orbitrap mass spectrometer coupled with an EASY-nLC 1200 system, as described recently.[15,16] The linear predictor of empirical RT from iRT[17] for targeted kinase peptides was

determined by the linear regression of RT versus iRT of tryptic peptides from BSA obtained for the chromatography setup prior to the analysis of kinase peptides.[9,15,16] This RT-iRT linear relationship was re-established between every eight LC-PRM runs by analyzing again the tryptic digestion mixture of BSA. The targeted precursor ions were monitored in eight separate injections for each sample in scheduled PRM mode with an 8-min retention time window.

All raw files were processed using Skyline (version 3.5) for the generation of extracted-ion chromatograms and for peak integration.[18] In this vein, the Skyline kinome PRM library includes MS/MS for peptides derived from approximately 400 kinase proteins, where up to four most abundant peptides were included for each kinase protein.[14] Six most abundant y ions found in MS/MS of each kinase peptide acquired from shotgun proteomic analysis were chosen for peptide identification and quantification, where a mass accuracy of 20 ppm or less was imposed for fragment ions during the identification of peptides in the Skyline platform. The targeted peptides were first manually checked to ensure the chromatographic profiles of multiple fragment ions derived from the light and heavy forms of the same peptide could be overlaid. The data were then processed to ensure that the distribution of the relative intensities of multiple transitions for the same precursor ion of kinase peptides was correlated with the theoretical distribution in the kinome MS/MS spectral library entry. The sum of peak areas from all transitions of light peptide or the corresponding heavy form was used for the quantification of the peptide.

TCGA and CCLE Data Analysis

OncoLnc was employed for the analysis of The Cancer Genome Atlas (TCGA) data for the correlation in mRNA expression between *PRPS2* and *MYC* genes.[19] Box plot and scatter plots for PRPS2 mRNA expression in CRC cell lines were generated from the data retrieved from The Cancer Cell Line Encyclopedia (CCLE) database (https://portals.broadinstitute.org/ccle), which included the gene expression data for more than 1000 cell lines representing 37 types of cancer.[20] The kinome map in the TOC Graphic was generated using online tool Peptracker (https://peptracker.com/epd/analytics/?show_plot).[21]

Western Blot

SW480 and SW620 cells were cultured in six-well plates and were lysed at 50–70% confluency. The protein concentrations in the lysates were determined using Bradford Assay (Bio-Rad). The whole cell lysate for each sample (10 μg) was denatured by boiling in Laemmli loading buffer and resolved by using SDS-PAGE. Subsequently, the proteins were transferred onto nitrocellulose membrane at 4 °C overnight. The resulting membrane was blocked with PBS-T (PBS with 0.1% Tween 20) containing 5% milk (Bio-Rad) at 4 °C for 6 h. The membrane was subsequently incubated, at 4 °C, with primary antibody overnight and then with secondary antibody at room temperature for 1 h. After thorough washing with PBS-T, the HRP signals were detected using Pierce ECL Western Blotting Substrate (Thermo).

Antibodies recognizing human AK2 (Santa Cruz Biotechnology, sc-374095, 1:2000 dilution), PRPS1/2/3 (Santa Cruz Biotechnology, sc-376440, 1:2000 dilution), IGF2R (Santa

Cruz Biotechnology, sc-14408, 1:1000 dilution), EGFR (Santa Cruz Biotechnology, sc-03, 1:10 000 dilution), and CHEK1 (Cell Signaling, #2360, 1:5000 dilution) were employed as primary antibodies for Western blot analysis. Horseradish peroxidase-conjugated antirabbit IgG, IRDye 680LT Goat anti-Mouse IgG (H+L), and donkey antigoat IgG-HRP were used as secondary antibodies. Membranes were also probed with antiactin antibody (Cell Signaling #4967, 1:10 000 dilution) to confirm equal loading of protein lysate.

Migration and Invasion Assay

Migration and invasion assays were performed using a Matrigel Transwell Chamber (Corning) with 8-μm pore polycarbonate filters.[22] In the migration assay, the harvested cells were suspended in 100 μL of serum-free medium at a final concentration of 1–2 × 10^6 cells/mL and were added to the upper chamber of the transwell system. Medium containing 10% FBS was placed in the lower chamber. After incubation for the indicated periods of time, nonmigrated cells and media in the upper chamber were removed by using a cotton swab and the migrated cells on the bottom surface of the insert membrane were fixed by incubating with 75% methanol at room temperature for 15 min. The cells were then stained with 0.2% crystal violet in 10% ethanol for 15 min. After washing and drying, the insert membranes were imaged under a light microscope. Since the same number of cells was initially dispersed in each well, cell migration was represented by the number of migrated cells.

In the invasion assay, 200–400 μg/mL matrigel in serum-free media was coated on the upper chamber of the filter and the matrigel-containing medium was removed after incubation at 37 °C for 2 h. The cells were then dispersed, stained, and counted in a similar way as described above for the migration assay. Cell invasion was calculated by dividing the number of invaded cells over that of the migrated cells.

Real-Time Quantitative PCR (RT-qPCR)

Cells were seeded in six-well plates at 50–70% confluence level. Total RNA was extracted from cells using TRI reagent (Sigma). Approximately 3 μg of RNA was reverse transcribed by employing M-MLV reverse transcriptase (Promega) and an oligo$(dT)_{18}$ primer. After a 60-min incubation at 42 °C, the reverse transcriptase was deactivated by heating at 75 °C for 5 min. RT-qPCR was performed using iQ SYBR Green Supermix kit (Bio-Rad) on a Bio-Rad iCycler system (Bio-Rad), and the running conditions were at 95 °C for 3 min and 45 cycles at 95 °C for 15 s, 55 °C for 30 s, and 72 °C for 45 s. The comparative cycle threshold (Ct) method (ΔΔCt) was used for the relative quantification of gene expression,[23] and the primer sequences are listed in Table S2.

Gelatin Zymography Assay

Concentrated medium collected from cultured CRC cells was loaded without reduction onto a 10% SDS-PAGE gel with 0.1% gelatin. After electrophoresis, the gels were washed with 2.5% Triton X-100 (Sigma) to remove SDS and to renature MMP-2 and MMP-9. The gels were subsequently incubated in the developing buffer for overnight to induce gelatin lysis by the renatured MMP-2 and MMP-9. The relative amounts of active MMP-2 and MMP-9 were then quantified based on their band intensities using ImageJ.[24]

RESULTS AND DISCUSSION

Differential Expression of Kinase Proteins in Primary and Metastatic Human CRC Cells

To explore the potential roles of kinases in CRC metastasis, we employed a PRM-based targeted proteomic method,[14] in conjunction with SILAC,[25] to examine the differential expression of kinases in a pair of matched primary/metastatic CRC cells, that is, SW480 and SW620 (Figure 1a), derived from the same CRC patient, respectively.[26]

The results from the PRM-based targeted proteomic method led to the quantification of 299 unique kinases in the paired CRC cells, which included more than 200 protein kinases and covered approximately 50% of the human kinome (Figure 2 and Table S1). The same retention time with dot product (dotp) being above 0.7 was displayed for all PRM transitions (4–6) used in kinase peptide quantification (Figure S1).[27] In addition, consistent trends were observed for more than 90% of the quantified kinase peptides in forward and reverse SILAC labeling experiments (Figure 1b and Figure 1c, Table S1, and representative results for AK2 and PRPS2 are shown in Figure 3a). We also validated the relative protein expression levels of five quantified kinases (AK2, CHEK1, EGFR, IGF2R, and PRPS2) in SW480 and SW620 cells by using Western blot analyses (Figure 3 and Figure S2). These results confirmed that LC-PRM analysis, together with SILAC labeling, provided robust quantification of kinase protein expression. In this respect, it is worth noting that the current LC-PRM method provides relative quantification of expression levels of kinase proteins in the paired SW480/SW620 cells; the method does not offer information about the absolute expression levels of kinase proteins (e.g., copy numbers of kinase molecules per cell). It can be envisaged that the method can be adapted for absolute quantification of kinase proteins in the future (e.g., with the use of stable isotope-labeled kinase peptides).[28]

Among the 299 quantified kinases, 83 and 77 were up- and down-regulated by at least 1.5-fold in the SW620 metastatic CRC cells relative to SW480 CRC cells, respectively. The failure in detecting the remaining kinases is likely due to their relatively low levels of expression or their lack of presence in our kinome PRM library, which contains ~80% of the human kinome.[14] Kyoto Encyclopedia of Genes and Genomes (KEGG) pathway analysis showed that 12 out of the 83 up-regulated kinases were involved in focal adhesion pathway (Figure S3a), which is closely associated with cancer metastasis.[29] Furthermore, both SRC and CSK in the SRC subfamily, which were previously shown to promote invasion of CRC cells,[30] were up-regulated in the metastatic SW620 cells (Figure 2, Table S1).

PRPS2 Drives CRC Metastasis

KEGG pathway analysis also reveals that 10 out of the 83 up-regulated kinases are involved in purine metabolism, rendering it one of the major up-regulated pathways (Figure S3a). Moreover, a previous study on metabolic reprograming of CRC also suggested that purine metabolism is activated in late-stage CRC patients.[31] Among these kinases, the mRNA expression of *PRPS2* gene is uniquely up-regulated in CRC cell lines among the more than 1000 cell lines representing 37 different cancer types in the Cancer Cell Line Encyclopedia (CCLE) database,[20] suggesting an important role of PRPS2 in CRC development (Figure S3b).

To further substantiate the above findings, we investigated the potential roles of PRPS2 in CRC metastasis by asking how the migration and invasion capacities of CRC cells are influenced by the expression levels of PRPS2.[22] Our results demonstrated that the migratory and invasive abilities of SW480 primary CRC cells were augmented upon overexpression of PRPS2 (Figures 4a,b and S4a). Reciprocally, shRNA-mediated stable knock-down of PRPS2 in SW620 metastatic CRC cells suppressed their motility and invasion (Figures 4c, S4b,c, and S5).

PRPS2 Modulates Expression of MMP-9 and E-Cadherin

Matrix metalloproteinases 2 and 9 (MMP-2 and MMP-9, a.k.a. gelatinases A and B) play central roles in degrading extracellular matrix (ECM) proteins and in promoting cancer metastasis.[32] Hence, we also asked whether the enzymatic activities of MMP-2 and MMP-9 are modulated by the expression levels of PRPS2. By employing gelatin zymography assay, [24] we showed that the activity of secreted MMP-9 from SW480 and SW620 cells were positively correlated with the expression level of PRPS2. In this regard, ectopic overexpression of PRPS2 in SW480 primary CRC cells gave rise to increased enzymatic activity of secreted MMP-9 (Figures 5a,b). Reciprocally, the activity of secreted MMP-9 was diminished in SW620 metastatic CRC cells upon stable knock-down of PRPS2 (Figure 5d,e). We also assessed, by employing RT-qPCR, how the mRNA expression levels of *MMP2* and *MMP9* genes in CRC cells are regulated by the expression levels of PRPS2. As shown in Figure 5c, ectopic overexpression of PRPS2 in SW480 primary CRC cells induced heightened mRNA expression of the *MMP9* gene, whereas stable knock-down of PRPS2 in the SW620 metastatic CRC cells suppressed the expression of *MMP9* gene (Figure 5f). However, the mRNA expression or activity of secreted MMP-2 is not positively modulated by PRPS2.

Aside from MMPs, epithelial-mesenchymal transition (EMT), a process through which cohesive epithelial cells are transformed to a migratory mesenchymal phenotype, can promote the invasion and metastasis of many types of cancer cells.[33] Along this line, EMT is accompanied with a loss of E-cadherin and a concomitant gain of N-cadherin.[34] E-Cadherin, which assumes important functions in cell–cell adhesion in epithelial tissues, is known to suppress malignant transformation.[35,36] Our data suggest that the expression of *CDH1* gene, which encodes E-cadherin, is inhibited by PRPS2 in CRC cells. Overexpression of PRPS2 in SW480 primary CRC cells inhibited the transcription of *CDH1* gene, whereas stable knockdown of PRPS2 in the metastatic SW620 cells stimulated the expression of *CDH1* gene (Figure 5c,f). Nevertheless, the expression of *CDH2* gene, which encodes N-cadherin, is not affected by PRPS2. Together, PRPS2 drives CRC metastasis by inhibiting the transcription of E-cadherin and promoting the expression and activities of MMP-9.

PRPS2 and Myc

We next explored the potential mechanism through which the elevated expression of PRPS2 stimulates CRC metastasis in cells. *MYC,* one of the most potent proto-oncogenes,[37,38] can promote tumorigenesis in various organs through altering cellular metabolism. PRPS2 is a crucial kinase in purine metabolism and protein synthesis.[39–41] Additionally, *MYC*-overexpressing cells often exhibit increased nucleotide biosynthesis through modulating the

expression of PRPS2.[41,42] Furthermore, elevated expression of *MYC* gene in CRC patients is known,[43] and the metabolic alteration of CRC is also induced by Myc.[31] Hence, we reason that the expression of PRPS2 in CRC cells could be modulated by Myc.

To examine the relationship between PRPS2 and Myc in CRC, we analyzed the expression of *PRPS2* and *MYC* in all 56 CRC cell lines included in the CCLE database. It turned out that the expression levels of *PRPS2* and *MYC* are well-correlated in CRC cell lines, including the SW480 and SW620 cells employed in the present study (Figure S6a). In this vein, the expression of *MYC* gene was previously shown to be elevated in SW620 cells relative to SW480 cells,[44] suggesting that the elevated expression of PRPS2 protein in SW620 cells could be modulated by Myc. Furthermore, the expression levels of *MYC* and *PRPS2* genes are also correlated with each other in 435 CRC patients in the TCGA database (Figure S6b), indicating that Myc may modulate the expression of PRPS2 in CRC cells and patients (Figure S7).

CONCLUSIONS

By employing a PRM-based targeted proteomic method, we were able to quantify the relative expression levels of 299 kinases in a pair of primary and metastatic CRC cells derived from the same patient. Importantly, we found that, among the differentially expressed kinases, PRPS2 promotes the migration and invasion of cultured CRC cells. Furthermore, we showed that elevated PRPS2 expression confers attenuated transcription of *CDH1* and augmented expression and activities of MMP-9. Moreover, our work supports the role of *MYC* proto-oncogene in up-regulating the *PRPS2* gene in metastatic CRC. Together, we discovered PRPS2 as a novel promoter for CRC metastasis.

Supplementary Material

Refer to Web version on PubMed Central for supplementary material.

ACKNOWLEDGMENTS

This work was supported by the National Institutes of Health (R01 CA210072).

REFERENCES

(1). Haggar FA; Boushey RP Colorectal Cancer Epidemiology: Incidence, Mortality, Survival, and Risk Factors. Clin. Colon Rectal. Surg. 2009, 22, 191–197. [PubMed: 21037809]

(2). Vatandoust S; Price TJ; Karapetis CS Colorectal cancer: Metastases to a single organ. World J. Gastroenterol. 2015, 21, 11767–11776. [PubMed: 26557001]

(3). Van Cutsem E; Oliveira J Advanced colorectal cancer: ESMO Clinical Recommendations for diagnosis, treatment and follow-up. Ann. Oncol. 2009, 20, 61–63. [PubMed: 19454465]

(4). Field K; Lipton L Metastatic colorectal cancer-past, progress and future. World J. Gastroenterol. 2007, 13, 3806–3815. [PubMed: 17657834]

(5). Warsinggih W; Yusuf I; Manuaba IBTW; Pusponegoro A Associations of positive epidermal growth factor receptor expression and K-RAS gene mutations with various clinicopathological parameters and survival of colorectal carcinoma patients. Biomarkers Genomic Med 2015, 7, 1–7.

(6). Uribe DJ; Mandell EK; Watson A; Martinez JD; Leighton JA; Ghosh S; Rothlin CV The receptor tyrosine kinase AXL promotes migration and invasion in colorectal cancer. PLoS One 2017, 12, No. e0179979. [PubMed: 28727830]

(7). Xiao Y; Guo L; Wang Y A targeted quantitative proteomics strategy for global kinome profiling of cancer cells and tissues. Mol. Cell. Proteomics 2014, 13, 1065–1075. [PubMed: 24520089]

(8). Patricelli MP; Szardenings AK; Liyanage M; Nomanbhoy TK; Wu M; Weissig H; Aban A; Chun D; Tanner S; Kozarich JW Functional Interrogation of the Kinome Using Nucleotide Acyl Phosphates. Biochemistry 2007, 46, 350–358. [PubMed: 17209545]

(9). Miao W; Xiao Y; Guo L; Jiang X; Huang M; Wang Y A high-throughput targeted proteomic approach for comprehensive profiling of methylglyoxal-induced perturbations of the human kinome. Anal. Chem. 2016, 88, 9773–9779. [PubMed: 27626823]

(10). Duncan JS; Whittle MC; Nakamura K; Abell AN; Midland AA; Zawistowski JS; Johnson NL; Granger DA; Jordan NV; Darr DB; Usary J; Kuan PF; Smalley DM; Major B; He X; Hoadley KA; Zhou B; Sharpless NE; Perou CM; Kim WY; Gomez SM; Chen X; Jin J; Frye SV; Earp HS; Graves LM; Johnson GL Dynamic reprogramming of the kinome in response to targeted MEK inhibition in triple-negative breast cancer. Cell 2012, 149, 307–21. [PubMed: 22500798]

(11). Stuhlmiller TJ; Miller SM; Zawistowski JS; Nakamura K; Beltran AS; Duncan JS; Angus SP; Collins KA; Granger DA; Reuther RA; Graves LM; Gomez SM; Kuan PF; Parker JS; Chen X; Sciaky N; Carey LA; Earp HS; Jin J; Johnson GL Inhibition of lapatinib-induced kinome reprogramming in ERBB2-positive breast cancer by targeting BET family bromodomains. Cell Rep. 2015, 11, 390–404. [PubMed: 25865888]

(12). Oppermann FS; Gnad F; Olsen JV; Hornberger R; Greff Z; Kéri G; Mann M; Daub H Large-scale proteomics analysis of the human kinome. Mol. Cell. Proteomics 2009, 8, 1751–1764. [PubMed: 19369195]

(13). Urisman A; Levin RS; Gordan JD; Webber JT; Hernandez H; Ishihama Y; Shokat KM; Burlingame AL An optimized chromatographic strategy for multiplexing In parallel reaction monitoring mass spectrometry: insights from quantitation of activated kinases. Mol. Cell. Proteomics 2017, 16, 265–277. [PubMed: 27940637]

(14). Miao W; Guo L; Wang Y Imatinib-Induced Changes in Protein Expression and ATP-Binding Affinities of Kinases in Chronic Myelocytic Leukemia Cells. Anal. Chem. 2019, 91, 3209–3214. [PubMed: 30773012]

(15). Miao W; Li L; Wang Y A targeted proteomic approach for heat shock proteins reveals DNAJB4 as a suppressor for melanoma metastasis. Anal. Chem. 2018, 90, 6835–6842. [PubMed: 29722524]

(16). Miao W; Li L; Wang Y Identification of helicase proteins as clients for HSP90. Anal. Chem. 2018, 90, 11751–11755. [PubMed: 30247883]

(17). Escher C; Reiter L; MacLean B; Ossola R; Herzog F; Chilton J; MacCoss MJ; Rinner O Using iRT, a normalized retention time for more targeted measurement of peptides. Proteomics 2012, 12, 1111–1121. [PubMed: 22577012]

(18). MacLean B; Tomazela DM; Shulman N; Chambers M; Finney GL; Frewen B; Kern R; Tabb DL; Liebler DC; MacCoss MJ Skyline: an open source document editor for creating and analyzing targeted proteomics experiments. Bioinformatics 2010, 26, 966–968. [PubMed: 20147306]

(19). Anaya J OncoLnc: linking TCGA survival data to mRNAs, miRNAs, and lncRNAs. PeerJ Comput. Sci. 2016, 2, No. e67.

(20). Barretina J; Caponigro G; Stransky N; Venkatesan K; Margolin AA; Kim S; Wilson CJ; Lehár J; Kryukov GV; Sonkin D; Reddy A; Liu M; Murray L; Berger MF; Monahan JE; Morais P; Meltzer J; Korejwa A; Jané-Valbuena J; Mapa FA; Thibault J; Bric-Furlong E; Raman P; Shipway A; Engels IH; Cheng J; Yu GK; Yu J; Aspesi P; de Silva M; Jagtap K; Jones MD; Wang L; Hatton C; Palescandolo E; Gupta S; Mahan S; Sougnez C; Onofrio RC; Liefeld T; MacConaill L; Winckler W; Reich M; Li N; Mesirov JP; Gabriel SB; Getz G; Ardlie K; Chan V; Myer VE; Weber BL; Porter J; Warmuth M; Finan P; Harris JL; Meyerson M; Golub TR; Morrissey MP; Sellers WR; Schlegel R; Garraway LA The Cancer Cell Line Encyclopedia enables predictive modelling of anticancer drug sensitivity. Nature 2012, 483, 603. [PubMed: 22460905]

(21). Brenes A; Lamond AI The encyclopedia of proteome dynamics: the kinoViewer. Bioinformatics 2018, 1–2.

(22). Albini A; Benelli R The chemoinvasion assay: a method to assess tumor and endothelial cell invasion and its modulation. Nat. Protoc. 2007, 2, 504. [PubMed: 17406614]

(23). Livak KJ; Schmittgen TD Analysis of relative gene expression data using real-time quantitative PCR and the 2^{-DDCt} method. Methods 2001, 25, 402–408. [PubMed: 11846609]

(24). Vandooren J; Geurts N; Martens E; Van den Steen PE; Opdenakker G Zymography methods for visualizing hydrolytic enzymes. Nat. Methods 2013, 10, 211–220. [PubMed: 23443633]

(25). Ong S-E; Blagoev B; Kratchmarova I; Kristensen DB; Steen H; Pandey A; Mann M Stable isotope labeling by amino acids in cell culture, SILAC, as a simple and accurate approach to expression proteomics. Mol. Cell. Proteomics 2002, 1, 376–386. [PubMed: 12118079]

(26). Leibovitz A; Stinson JC; McCombs WB; McCoy CE; Mazur KC; Mabry ND Classification of Human Colorectal Adenocarcinoma Cell Lines. Cancer Res. 1976, 36, 4562. [PubMed: 1000501]

(27). de Graaf EL; Altelaar AF; van Breukelen B; Mohammed S; Heck AJ Improving SRM assay development: a global comparison between triple quadrupole, ion trap, and higher energy CID peptide fragmentation spectra. J. Proteome Res. 2011, 10, 4334–4341. [PubMed: 21726076]

(28). Gerber SA; Rush J; Stemman O; Kirschner MW; Gygi SP Absolute quantification of proteins and phosphoproteins from cell lysates by tandem MS. Proc. Natl. Acad. Sci. U. S. A. 2003, 100, 6940–6945. [PubMed: 12771378]

(29). Bijian K; Lougheed C; Su J; Xu B; Yu H; Wu JH; Riccio K; Alaoui-Jamali MA Targeting focal adhesion turnover in invasive breast cancer cells by the purine derivative reversine. Br. J. Cancer 2013, 109, 2810. [PubMed: 24169345]

(30). Sirvent A; Bénistant C; Pannequin J; Veracini L; Simon V; Bourgaux JF; Hollande F; Cruzalegui F; Roche S Src family tyrosine kinases-driven colon cancer cell invasion is induced by Csk membrane delocalization. Oncogene 2010, 29, 1303. [PubMed: 20010872]

(31). Satoh K; Yachida S; Sugimoto M; Oshima M; Nakagawa T; Akamoto S; Tabata S; Saitoh K; Kato K; Sato S; Igarashi K; Aizawa Y; Kajino-Sakamoto R; Kojima Y; Fujishita T; Enomoto A; Hirayama A; Ishikawa T; Taketo MM; Kushida Y; Haba R; Okano K; Tomita M; Suzuki Y; Fukuda S; Aoki M; Soga T Global metabolic reprogramming of colorectal cancer occurs at adenoma stage and is induced by MYC. Proc. Natl. Acad. Sci. U. S. A. 2017, 114, E7697–E7706. [PubMed: 28847964]

(32). Bauvois B New facets of matrix metalloproteinases MMP-2 and MMP-9 as cell surface transducers: outside-in signaling and relationship to tumor progression. Biochim. Biophys. Acta, Rev. Cancer 2012, 1825, 29–36.

(33). Thiery JP Epithelial–mesenchymal transitions in tumour progression. Nat. Rev. Cancer 2002, 2, 442. [PubMed: 12189386]

(34). Kalluri R; Weinberg RA The basics of epithelial-mesenchymal transition. J. Clin. Invest. 2009, 119, 1420–1428. [PubMed: 19487818]

(35). Pećina-Šlaus N Tumor suppressor gene E-cadherin and its role in normal and malignant cells. Cancer Cell Int. 2003, 3, 17–17a. [PubMed: 14613514]

(36). Gumbiner BM Cell Adhesion: The Molecular Basis of Tissue Architecture and Morphogenesis. Cell 1996, 84, 345–357. [PubMed: 8608588]

(37). Stone J; de Lange T; Ramsay G; Jakobovits E; Bishop JM; Varmus H; Lee W Definition of regions in human c-myc that are involved in transformation and nuclear localization. Mol. Cell. Biol. 1987, 7, 1697. [PubMed: 3299053]

(38). Hemann MT; Bric A; Teruya-Feldstein J; Herbst A; Nilsson JA; Cordon-Cardo C; Cleveland JL; Tansey WP; Lowe SW Evasion of the p53 tumour surveillance network by tumour-derived MYC mutants. Nature 2005, 436, 807. [PubMed: 16094360]

(39). Miller DM; Thomas SD; Islam A; Muench D; Sedoris K c-Mycand CancerMetabolism. Clin. CancerRes. 2012, 18, 5546–5553.

(40). Rochlitz CF; Herrmann R; de Kant E Overexpression and Amplification of *c-myc* during Progression of Human Colorectal Cancer. Oncology 2004, 53, 448–454.

(41). Cunningham JT; Moreno MV; Lodi A; Ronen SM; Ruggero D Protein and nucleotide biosynthesis are coupled by a single rate-limiting enzyme, PRPS2, to drive cancer. Cell 2014, 157, 1088–1103. [PubMed: 24855946]

(42). Mannava S; Grachtchouk V; Wheeler LJ; Im M; Zhuang D; Slavina EG; Mathews CK; Shewach DS; Nikiforov MA Direct role of nucleotide metabolism in C-MYC-dependent proliferation of melanoma cells. Cell Cycle 2008, 7, 2392–2400. [PubMed: 18677108]

(43). Smith DR; Myint T; Goh HS Over-expression of the c-myc proto-oncogene in colorectal carcinoma. Br. J. Cancer 1993, 68, 407–413. [PubMed: 8347498]

(44). Grand CL; Powell TJ; Nagle RB; Bearss DJ; Tye D; Gleason-Guzman M; Hurley LH Mutations in the G-quadruplex silencer element and their relationship to c-MYC overexpression, NM23 repression, and therapeutic rescue. Proc. Natl. Acad. Sci. U. S. A. 2005, 102, 516.

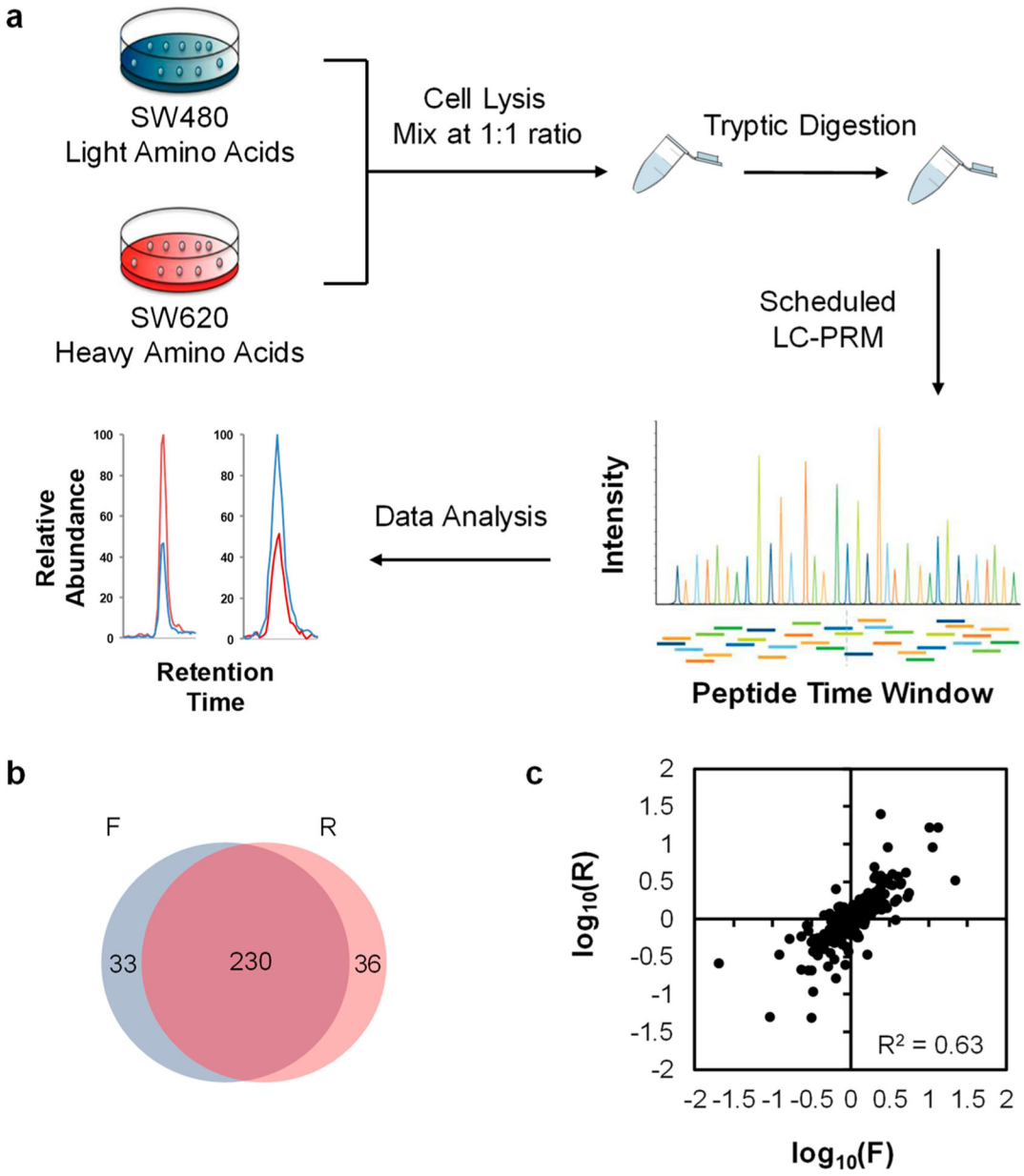

Figure 1.

PRM-based targeted proteomic approach for interrogating the perturbations in protein expression levels of kinases during CRC metastasis (a) Experimental strategy for PRM-based targeted proteomic approach. (b) Venn diagram displaying the overlap between quantified kinases from the forward and reverse SILAC labelings of the SW480/SW620 pair of CRC cells. (c) Correlation between the ratios of kinase protein expression in SW480/SW620 cells obtained from forward and reverse SILAC labeling experiments.

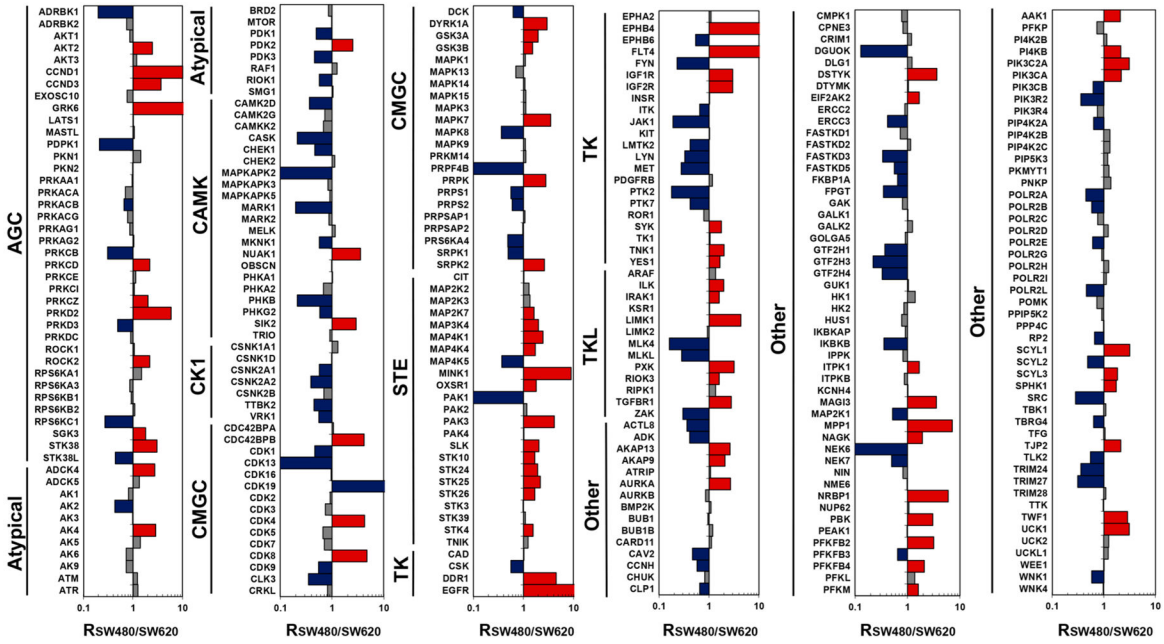

Figure 2.

Differential expression of kinase proteins in paired SW480/SW620 CRC cells. Blue, red, and gray bars represent those kinases with ratios (SW480/SW620) that are <0.67, >1.5, and between 0.67 and 1.5, respectively.

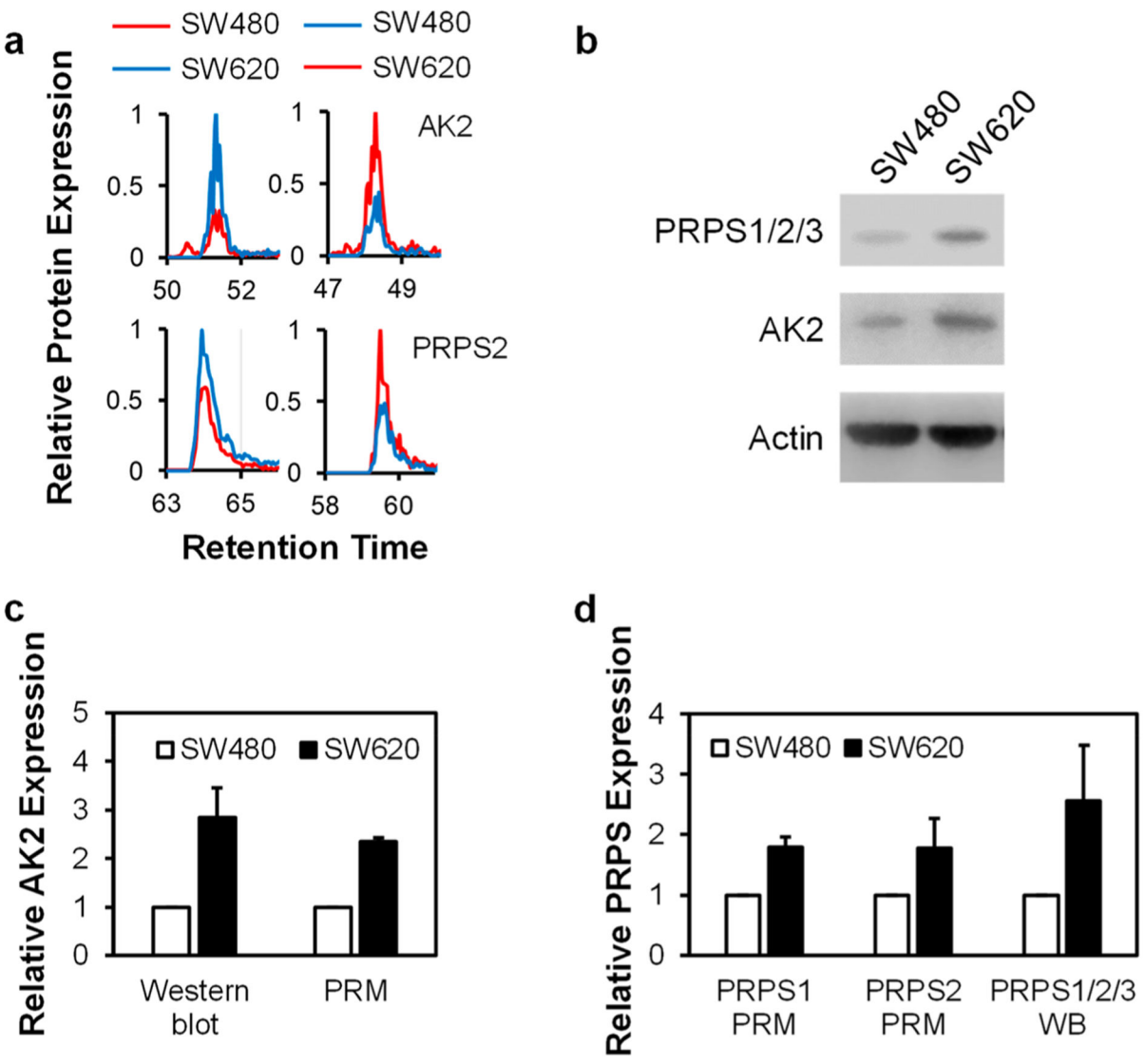

Figure 3.

AK2 and PRPS2 are up-regulated in metastatic CRC cells. (a) PRM traces for the quantifications of AK2 and PRPS2 proteins in SW480/SW620 cells. (b) Western blot for the validation of the expression levels of AK2 and PRPS proteins in the paired CRC cells. (c) Quantitative comparison of the ratios of AK2 obtained from PRM and Western blot analysis. (d) Quantitative comparison of the ratios of PRPS proteins obtained from PRM (for PRPS1 and PRPS2) and Western blot analysis (for PRPS1/2/3). The data represent the mean ± S.D. of the quantification results ($n = 3$).

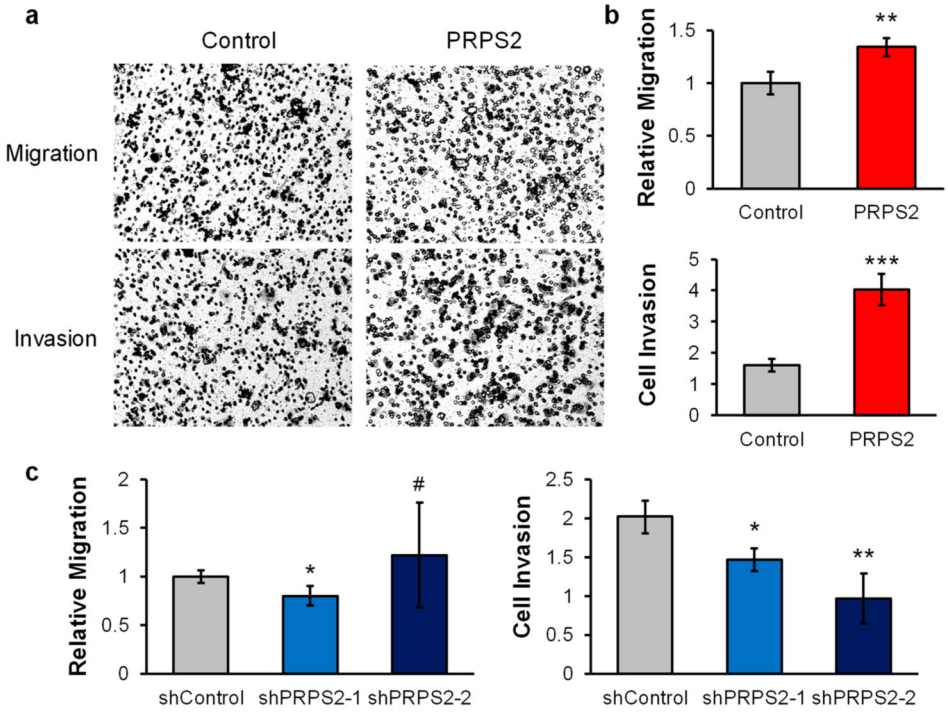

Figure 4.

PRPS2 modulates the migratory and invasive capacities of CRC cells. (a) Migratory and invasive abilities of SW480 primary colorectal cancer cells were increased upon ectopic overexpression of PRPS2. (b,c) Quantification results of migratory and invasive abilities of SW480 primary colorectal cancer cells upon ectopic overexpression of *PRPS2* gene (b), and those of SW620 metastatic colorectal cancer cells upon shRNA-mediated stable knock-down of *PRPS2* gene (c), respectively. The data represent the mean ± S. D. of the quantification results ($n = 3$). The p values were calculated using unpaired, two-tailed Student's t-test: #, $p \geq 0.05$; *, $0.01 \leq p < 0.05$; **, $0.001 \leq p < 0.01$; ***, $p < 0.001$.

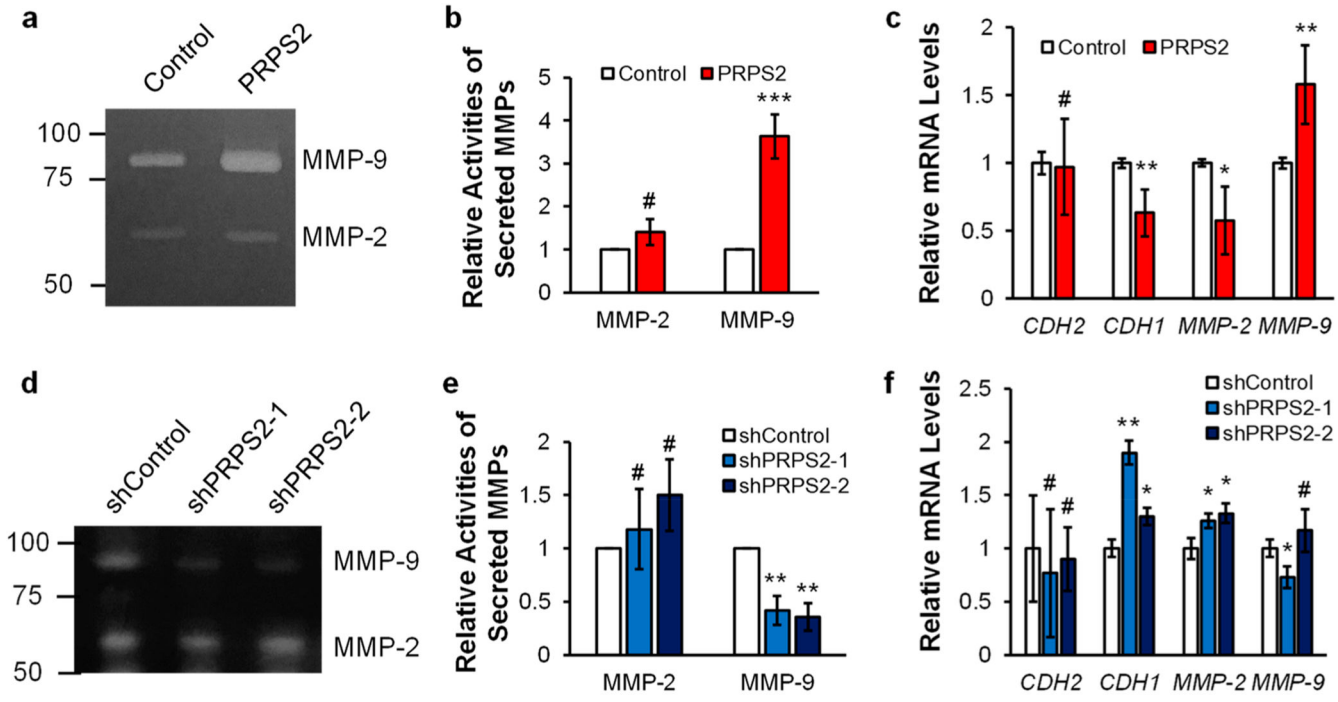

Figure 5.

PRPS2 regulates the expression and enzymatic activity of MMP-9. (a) Gelatin zymography assay showing the changes in activities of secreted MMP-2 and MMP-9 upon ectopic overexpression of PRPS2 in SW480 cells. (b) Modulation of activities of secreted MMP-2 and MMP-9 by PRPS2 in SW480 cells. (c) RT-qPCR results showing the changes in mRNA levels of *CDH2* (encoding N-cadherin), *CDH1* (encoding E-cadherin), *MMP2,* and *MMP9* genes in SW480 cells upon ectopic overexpression of PRPS2. (d) Gelatin zymography assay showing the changes in activities of secreted MMP-2 and MMP-9 after shRNA-mediated stable knock-down of *PRPS2* gene in SW620 cells. (e) Modulation of activities of secreted MMP-2 and MMP-9 by PRPS2 in SW620 cells. (f) RT-qPCR results showing the modulation in mRNA levels of *CDH2, CDH1, MMP2,* and *MMP9* genes in SW620 cells upon siRNA-mediated knockdown of PRPS2. The data represent the mean ± S. D. of the quantification results ($n = 3$). The p values were calculated based on unpaired, two-tailed Student's t-test: #, $p \geq 0.05$; *, $0.01 \leq p < 0.05$; **, $0.001 \leq p < 0.01$; ***, $p < 0.001$.